Enhanced laser cooling of CO_2–Xe gas using (02^00) excitation

Seungha Shin and Massoud Kaviany[a)]
Department of Mechanical Engineering, University of Michigan, Ann Arbor, Michigan 48109-2125, USA

(Received 2 September 2009; accepted 13 November 2009; published online 30 December 2009)

Laser irradiation with a 9.6 μm wavelength resonant with the (02^00) level improves the anti-Stokes cooling of CO_2 gas. Excitation of the (02^00) level increases cooling by producing a larger population of (00^01), despite the higher-energy photon absorption, compared to a (10^00) level excitation. Further selection of macroconditions (temperature, pressure, Xe diluent atomic fraction, and geometric parameters) enhances cooling by reducing parasite gas conduction through slower thermal energy transport and increasing the nonequilibrium population of the excited (00^01) level by fast species diffusion and small collisional relaxation. We include reabsorption, and then find the conditions for optimal cooling. © *2009 American Institute of Physics*. [doi:10.1063/1.3273488]

I. INTRODUCTION

While a number of studies have been published on atomic gas laser cooling[1–4] for trapped ultracold atoms, studies on molecular-gas laser cooling have been rather limited in number.[5,6] Cooling of molecules such as the alkaline-earth monohydrides via magneto-optical trapping has been suggested;[7] several other attempts have been made to produce ultracold gaseous molecules, but so far they have not been successful.[8] Kinetic cooling has also been suggested and observed with CO_2 and other molecules, but it is only transient with negligible cooling.[9,10] So far, the only successful net cooling of molecular gases has been achieved in CO_2 gas cooling by the anti-Stokes fluorescence.[11] However, this cooling only reached 1 K at 600 K using 10.6 μm CO_2 laser irradiation with Xe as the diluent. Here, we select an excitation laser with a shorter wavelength in molecular-gas anti-Stokes cooling system and find cooling enhancement and the optimal cooling conditions. Since no mechanical means is needed and cooling is achieved much faster (compared, for example, to expansion cooling of gas streams), laser cooling of molecular gases is attractive, although it does not yield an ultracold gas. Laser irradiation leads to a nonequilibrium population distribution of molecular gas. Laser cooling can exploit low-entropy nonequilibrium population distribution (before it equilibrates and increases entropy). This study aims at manipulation of nonequilibrium population to enhance energy conversion.

Molecular-gas laser cooling employs vibrational states, in contrast to solid-state anti-Stokes laser cooling, which uses doped-ion electronic energy levels and phonons.[12] The Herzberg[13] notation, $(v_1v_2^lv_3)$, is used for vibrational states, where v_1, v_2, and v_3 are the symmetric, bending, and asymmetric vibrational quantum numbers and l is the angular quantum number of the bending mode. Because the population of overtone vibration levels is low at low vibration temperatures, only levels under (00^01) are considered. Among these, (00^00), (10^00), and (02^00) are possible levels for radiative excitation to (00^01), according to the vibration mode transition selection rule.[14] Covering the above-mentioned levels, in this analysis, we assume a five-level vibration energy system, as shown in Fig. 1(a).[13] Compared to the three-level analysis in Ref. 11, we consider other possible resonant irradiations that allow selections of other laser frequencies and expect more accurate results and predictions using this energy level system.

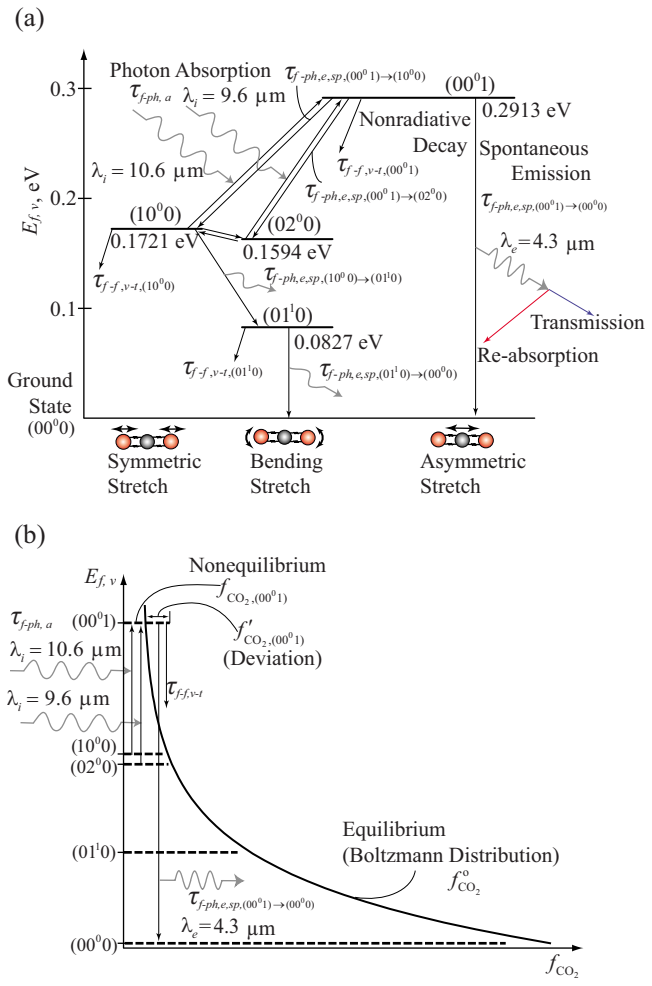

FIG. 1. (Color online) (a) Five-level vibrational energy transitions and their time constants in laser cooling of CO_2 gas. (b) Equilibrium and nonequilibrium population distributions of CO_2 vibrational modes in laser cooling. The photon wavelength is selected to transitions with the most effective cooling.

[a)]Electronic mail: kaviany@umich.edu.

The addition of Xe improves cooling by lowering the mixture thermal conductivity and deactivating collisional relaxation.[15] At high temperatures, Ne, Ar, Kr, and He have larger deactivation effects than Xe,[16] but Xe lowers the mixture thermal conductivity[17] due to its heavy atomic mass. Thus, Xe is still considered the most effective diluent for gas cooling. The gas mixture is contained in a long cylinder of radius R_t and irradiated with a laser beam of radius R_l traveling at the cylinder center.

II. ANALYSIS

A. Population distribution

We assume that the CO_2–Xe gas mixture system is in equilibrium before laser irradiation. All kinetic temperatures (vibrational, rotational, and translational) are therefore equal. The population of each vibration level generally follows the Boltzmann distribution. The population of energy level $(v_1 v_2^l v_3)$ is proportional to

$$f^{\mathrm{o}}_{v_1 v_2^l v_3} = \exp\left(-\frac{\Delta E_{v_1 v_2^l v_3}}{k_{\mathrm{B}} T}\right), \tag{1}$$

where k_{B} is the Boltzmann constant, $\Delta E_{v_1 v_2^l v_3}$ is the energy difference between the vibrational level $(v_1 v_2^l v_3)$ and ground level $(00^0 0)$, and T is the gas mixture temperature. Since the bending mode of CO_2 molecule is doubly degenerated, the vibration partition function becomes[18]

$$Z_{f,v} = (1 - f^{\mathrm{o}}_{10^0 0})^{-1}(1 - f^{\mathrm{o}}_{01^1 0})^{-2}(1 - f^{\mathrm{o}}_{00^0 1})^{-1}. \tag{2}$$

Thus the population density of energy level $(v_1 v_2^l v_3)$ is

$$n_{v_1 v_2^l v_3} = n_{\mathrm{CO_2}} f^{\mathrm{o}}_{v_1 v_2^l v_3} g_{v_1 v_2^l v_3} / Z_{f,v}, \tag{3}$$

where $g_{v_1 v_2^l v_3}$ is the degeneracy of the level $(v_1 v_2^l v_3)$ and $n_{\mathrm{CO_2}}$ is the population density of CO_2. Photon absorption causes a deviation in population distribution from the Boltzmann distribution. In this analysis, $(00^0 1)$ becomes populated by laser irradiation; the populated $(00^0 1)$ level then decays, emitting larger-energy photons with a large spontaneous relaxation rate when compared to the nonradiative decay. Cooling is thus achieved by generating the nonequilibrium, asymmetric $(00^0 1)$ level population fraction designated by $f_{\mathrm{CO_2},(00^0 1)}$ in Fig. 1(b).

B. Temperature distribution

Using symmetry, only the radial variations in temperature and species concentration are considered in this study. The laser beam is smaller than the cylinder, and therefore excited CO_2 molecules diffuse outward, as governed by their mass diffusivity. We use a dimensionless form of the steady-state temperature distribution given in Ref. 11 with the excited-population penetration length defined as

$$\delta_D = (D_f \tau_{f-\mathrm{ph}-f,(00^0 1)})^{1/2}, \tag{4}$$

where D_f is the mass diffusivity for the excited $(00^0 1)$ state and $\tau_{f-\mathrm{ph}-f,(00^0 1)}$ is the overall relaxation time of the $(00^0 1)$ state including radiative and nonradiative relaxations. The dimensionless cylinder and beam radii are $R_t^* = R_t/\delta_D$ and $R_l^* = R_l/\delta_D$. The reference temperature difference found from the energy equation is

$$\Delta T_{\mathrm{o}} = [n_{\mathrm{CO_2},(00^0 1),\mathrm{o}} \delta_D^2 (\mathrm{d}E_{c,h}/\mathrm{d}t)]/k_f, \tag{5}$$

where k_f is the gas thermal conductivity, $n_{\mathrm{CO_2},(00^0 1),\mathrm{o}}$ is the number density of the $(00^0 1)$ state in the irradiated beam region, and $\mathrm{d}E_{c,h}/\mathrm{d}t$ is the cooling/heating rate (cooling <0). This rate is uniform in the irradiated region if reabsorption of the 4.3 μm spontaneous emission is not considered. Thus, dimensionless cooling is

$$\frac{\Delta T(r^*)}{\Delta T_{\mathrm{o}}} = 2R_t^{*2} \times \sum_{n=1}^{\infty} \frac{\int_0^{\beta} r^* \mathrm{J_o}(\alpha_n r^*)\mathrm{d}r^* + \left[\int_{\beta}^{1} r^* \mathrm{K_o}(r^* R_l^*)\mathrm{J_o}(\alpha_n r^*)\mathrm{d}r^* / \mathrm{K_o}(R_l^*)\right]}{\alpha_n^2 [\mathrm{J_1}(\alpha_n)]^2}, \tag{6}$$

where α_n represents roots of the Bessel function $\mathrm{J_o}$, $\beta = R_l/R_t$ is the ratio of beam to cylinder radius, and $r^* = r/R_t$ is the dimensionless radial position. For $\beta = 1$, there is no spatial variation in $n_{\mathrm{CO_2},(00^0 1)}$, i.e., $\Delta T(r^*)$ is independent of D_f. Cooling is enhanced using large ΔT_{o}, i.e., small energy transport k_f, large species diffusion D_f, large nonequilibrium population $n_{\mathrm{CO_2},(00^0 1),\mathrm{o}}$, and large quantum efficiency.

C. Transition kinetics

Gas species diffusion and thermal energy transport are controlled by transition kinetics and the molecular kinetics (represented by D_f and k_f) of the gas mixture.[17,19–21] With a constant total number density, slow relaxation and large pumped molecules are desirable for maintaining large deviations from the equilibrium population across the cylinder. Relaxation of the $(00^0 1)$ level $\tau_{f-\mathrm{ph}-f,(00^0 1)}$ involves spontaneous emission $\tau_{f-\mathrm{ph},e,\mathrm{sp}}$ and nonradiative decay $\tau_{f-f,v-t}$ through vibration-translation or vibration-vibration energy transport (by collisions between CO_2 and CO_2 or CO_2 and Xe). The spontaneous emission rate for transition from i to j state is[22]

$$\tau^{-1}_{f-\mathrm{ph},e,\mathrm{sp},i-j} = \frac{64\pi^4 f^3_{e,g} |\mu_{e,i-j}|^2}{3 h_{\mathrm{P}} u^3_{\mathrm{ph}}}, \tag{7}$$

where $f_{e,g}$ is the emitted frequency, u_{ph} is the photon speed, h_{P} is the Planck constant, and $|\mu_{e,i-j}|$ is the transition dipole moment between the i and j states. Transition dipole moments have been estimated by *ab initio* calculations;[23] here we use the dipole moment from the measured absorption coefficient because of the higher accuracy.[24]

The time constant of the collisional nonradiative process $\tau_{f-f,v-t}$ is[25]

$$\tau_{f-f,v-t} = \frac{\tau_{f-f}}{P_{f-f,v-t}}, \tag{8}$$

where τ_{f-f} is the time constant of the molecular collision (from molecular kinetics)[22] and $P_{f-f,v-t}$ is the transition probability per collision estimated using a combination of experimental results[15,16,26] and theoretical models [Landau–Teller[27] and Schwartz-Slawsky-Herzfeld (SSH) (Ref. 25)]. During

collisional energy transport, relaxations are allowed from (00^01) to all lower levels $(v_1v_2^l0)$. Transitions to the closest levels [such as (11^10) and (04^00)] dominate (00^01) relaxation despite its small mole fraction because a transition with a large energy exchange has a low probability.[28] Adding dilutent Xe lowers the probability of (00^01) nonradiative relaxation because of the large collisional reduced mass and because Xe only has translational energy. The addition of Xe also increases relaxation rates in the lower levels.[15,29] The nonradiative relaxation time of a CO_2–Xe gas mixture, generally dependent on pressure p, is reported in Ref. 26

$$(p\tau_{f-f,v-t})^{-1} = x_{CO_2}(p\tau_{f-f,v-t,CO_2-CO_2})^{-1} + x_{Xe}(p\tau_{f-f,v-t,CO_2-Xe})^{-1}, \quad (9)$$

where x_{CO_2} and x_{Xe} are the mole fractions of Xe and CO_2, $\tau_{f-f,v-t,CO_2-CO_2}$ is the relaxation time constant by collisions between CO_2 molecules, and $\tau_{f-f,v-t,CO_2-Xe}$ is the relaxation time constant by collisions between CO_2 and Xe. From the time constants of nonradiative and radiative decays, the overall relaxation time of (00^01) is found as follows by the Matthiessen rule,

$$\tau_{f-ph-f,(00^01)}^{-1} = \sum \tau_{f-f,v-t,A-B,(00^01)}^{-1} + \sum \tau_{f-ph,e,sp,(00^01)\to(v_1v_2^l0)}^{-1}. \quad (10)$$

The (00^01) level population in the beam region also varies according to photon absorption rate and pumped-level population (10^00) or (02^00). Lower levels have larger populations according to the equilibrium Boltzmann distribution, so resonant irradiation with transition between the lower (02^00) and (00^01) levels leads to a larger number density for (00^01). Absorption and gain coefficients for the transition between (02^00) with rotational level j and (00^01) with j' are derived from stimulated absorption and emission rates. Using the time constant for spontaneous emission in decay from (02^00) and (00^01), these are[30]

$$\sigma_{ph,a,(02^00),j\to(00^01),j'} = \frac{n_{CO_2,(02^00)}}{\tau_{f-ph,e,sp,(00^01)\to(02^00)}\int_\omega d\omega} \times \frac{g_{(00^01),j'}}{g_{(02^00),j}}\left(\frac{\pi u_{ph}}{\omega_{(00^01)\to(02^00)}}\right)^2,$$

$$\sigma_{ph,g,(00^01),j'\to(02^00),j} = \frac{n_{CO_2,(00^01)}}{\tau_{f-ph,e,sp,(00^01)\to(02^00)}\int_\omega d\omega} \times \left(\frac{\pi u_{ph}}{\omega_{(00^01)\to(02^00)}}\right)^2, \quad (11)$$

where $\int_\omega d\omega$ is over a small bandwidth centered around $\omega_{(00^01)\to(02^00)}$, $g_{(02^00),j}$ and $g_{(00^01),j'}$ are the degeneracies of rotational levels of (02^00) and (00^01), and $n_{CO_2,(02^00)}$ and $n_{CO_2,(00^01)}$ are the number densities of (02^00) and (00^01). From the absorption relation (the Bouguer law), the rate equation under laser irradiation is

TABLE I. Time constants in laser cooling of CO_2–Xe gas.

Mechanism	Time constant	Magnitude
Radiative decay[a]	$\tau_{f-f,e,sp,(00^01)\to(00^00)}$	2.383 ms
	$\tau_{f-f,e,sp,(00^01)\to(02^00)}$	2172
	$\tau_{f-f,e,sp,(00^01)\to(10^00)}$	2378
	$\tau_{f-f,e,sp,(01^10)\to(00^00)}$	326.3
Nonradiative decay[b]	$p\tau_{f-f,v-t,CO_2-CO_2,(00^01)}$ [c]	3.06 ms torr
	$p\tau_{f-f,v-t,CO_2-CO_2,(10^00)}$ [d]	0.454
	$p\tau_{f-f,v-t,CO_2-CO_2,(01^10)}$ [d]	5.18
	$p\tau_{f-f,v-t,CO_2-Xe,(00^01)}$ [d]	33.3

[a]Calculated using transition dipole values from Ref. 24.
[b]Data for 300 K and data for other temperatures estimated using combination of experimental results (Refs. 15, 16, and 26) and theoretical models [Landau–Teller (Ref. 27) and SSH (Ref. 25)].
[c]Reference 26.
[d]Reference 15.

$$\frac{dn_{CO_2,(00^01)}}{dt} = -\frac{n_{CO_2,(00^01)}}{\tau_{f-ph-f,(00^01)}} + I_{ph}\left(\frac{\sigma_{ph,a,(02^00),j\to(00^01),j'}}{\hbar\omega_{(00^01)\to(02^00)}} - \frac{\sigma_{ph,g,(00^01),j'\to(02^00),j}}{\hbar\omega_{(00^01)\to(02^00)}}\right), \quad (12)$$

where I_{ph} is the laser intensity. Even though here we address laser irradiation causing rotational transition and population deviation for levels j and j', the populations of all rotational levels in (02^00) and (00^01) are affected by irradiation (due to the fast relaxation of the rotational levels). Thus, the absorption and emission rates by laser irradiation depend on I_{ph} and vibration population distribution. When we select a 9.6 μm wavelength laser on the P(28) line, which is the strongest transition in the group,[31] and I_{ph} is larger than 100 W/cm^2, these rates are much higher than the overall relaxation, and the excited-level population can be saturated close to the pumped energy level (99.99%). Therefore, the net absorption time constant $\tau_{f-ph,a}$ is limited to $\tau_{f-ph-f,(00^01)}$ under steady state.

The essential time constants for this analysis are shown in Table I. The transition from (00^01) to (00^00) has the largest spontaneous decay rate, and this radiative relaxation is faster than nonradiative decay under very low pressure. Hence, high occupancy of the (00^01) level under the low pressure with a properly selected Xe concentration is desirable for effective cooling.

D. Reabsorption

The cooling/heating rate is the difference between the absorbed photons under an overall relaxation rate and the photon emission rate by spontaneous processes. However, not all emitted photons from excited molecules reach the cylinder wall (once they reach there, it is assumed that they are completely absorbed). The average gas absorptance of the emitted photon depends on the integrated product of the absorption coefficient and path length, i.e.,

$$\langle \alpha_{\mathrm{ph},a,(00^00)\rightarrow(00^01)}(r)\rangle = \frac{1}{4\pi}\int_{\varphi=0}^{2\pi}\int_{\theta=0}^{\pi}\{1-\exp[-\sigma_{\mathrm{ph},a,(00^00)\rightarrow(00^01)} \times l_{\mathrm{ph}}(r,\theta,\varphi)]\}\sin\theta \mathrm{d}\theta\mathrm{d}\varphi, \quad (13)$$

where $\sigma_{\mathrm{ph},a,(00^00)\rightarrow(00^01)}$ is the absorption coefficient of a 4.3 μm wavelength and $l_{\mathrm{ph}}(r,\theta,\varphi)$ is the photon path length at radial position r and angular directions θ and φ. We only consider reabsorption of the 4.3 μm emission, which has the largest absorption cross-section area (from the Pacific Northwest National Laboratory (PNNL) database) and the highest spontaneous emission rate. Radiative decay rates of other spontaneous emissions are negligible compared to this. $\sigma_{\mathrm{ph},a,(00^00)\rightarrow(00^01)}$ is the product of the average absorption cross-section area (considering all branches in transition of rotational levels) $A_{\mathrm{ph},a,(00^00)\rightarrow(00^01)}$ and the number density difference in CO_2 molecules involved in the absorption process, $n_{\mathrm{CO}_2,(00^00)}-n_{\mathrm{CO}_2,(00^01)}$. Thus $\sigma_{\mathrm{ph},a,(00^00)\rightarrow(00^01)}$ increases with an increase in pressure and a decrease in temperature. The cooling/heating rate then becomes[32]

$$\frac{\mathrm{d}E_{c,h}(r)}{\mathrm{d}t} = \frac{\hbar\omega_i}{\tau_{f-\mathrm{ph}-f,(00^01)}} - \frac{\Sigma\hbar\omega_{(00^01)\rightarrow(v_1v_2^l0)}}{\tau_{f-\mathrm{ph},e,\mathrm{sp},(00^01)\rightarrow(v_1v_2^l0)}} + \frac{\langle\alpha_{\mathrm{ph},a,(00^00)\rightarrow(00^01)}(r)\rangle\hbar\omega_{(00^01)\rightarrow(00^00)}}{\tau_{f-\mathrm{ph},e,\mathrm{sp},(00^01)\rightarrow(00^00)}}, \quad (14)$$

where ω_i is the absorbed photon wavelength.

III. RESULTS AND DISCUSSION

In spite of the slightly larger photon energy absorption and lower absorption rate due to the smaller transition dipole, when compared to 10.6 μm,[24] we found that 9.6 μm resonance with excitation of (02^00) enhances cooling because of the increase in pumped population. The 10.6 and 9.6 μm dual-beam irradiations appear to raise the excited population, but the (00^01) level population cannot exceed the saturated population with a 9.6 μm irradiation. Also, dual irradiation with the 15 μm laser changes the population of other energy levels that have smaller radiative relaxation rates (compared to nonradiative), and this deteriorates cooling. The cooling enhancement of the 9.6 μm wavelength in Fig. 2 shows 3.93 K cooling at a cylinder temperature of 504 K, and 1.05 K with the cylinder at room temperature. All macroscopic conditions are the same as in Ref. 11, and the experimental result of Ref. 11 is also shown in Fig. 2. Comparison of laser wavelengths shows that the shorter wavelength results in improved cooling.

Even though k_f and $P_{f-f,v-t}$ increases at higher temperatures, pumped energy level (02^00) population also rises with an increase in (00^01). Higher temperatures increase D_f and maintain a large deviation in (00^01), even in the nonirradiated region. Higher temperatures decrease $\sigma_{\mathrm{ph},a,(00^00)\rightarrow(00^01)}$ due to a decrease in CO_2 number density. The maximum cooling temperature is found when the deteriorating factors—i.e., increased k_f and $P_{f-f,v-t}$—are properly compensated by the enhancing factors, i.e., large $n_{\mathrm{CO}_2,(00^01)}$, D_f, and small $\sigma_{\mathrm{ph},a,(00^00)\rightarrow(00^01)}$. Figures 3(a) and 3(b) show cooling variations with respect to macroscopic conditions: (a) pressure p and (b) Xe diluent atomic fraction x_{Xe}; both show optima. Low total pressures reduce reabsorption and nonradiative relaxation, but high pressures are desirable for significant species diffusion. Likewise, the larger x_{Xe} leads to lower k_f, larger D_f, smaller $\sigma_{\mathrm{ph},a}$, and lower $P_{f-f,v-t}$, while the smaller x_{Xe} the larger $n_{\mathrm{CO}_2,(00^01)}$.

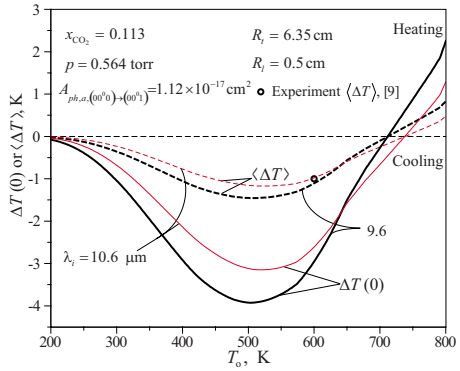

FIG. 2. (Color online) Comparison of 9.6 and 10.6 μm wavelength laser cooling, showing variations in cooling with respect to cylinder temperature for both wavelengths. The macroscopic conditions are the same as Ref. 11 and the experimental result of Ref. 11 for λ_i=10.6 μm is also shown.

As the cylinder radius R_t increases, the heat flow rate from the wall decreases, and reabsorption increases due to the longer photon path length. Selection of optimal R_t is also

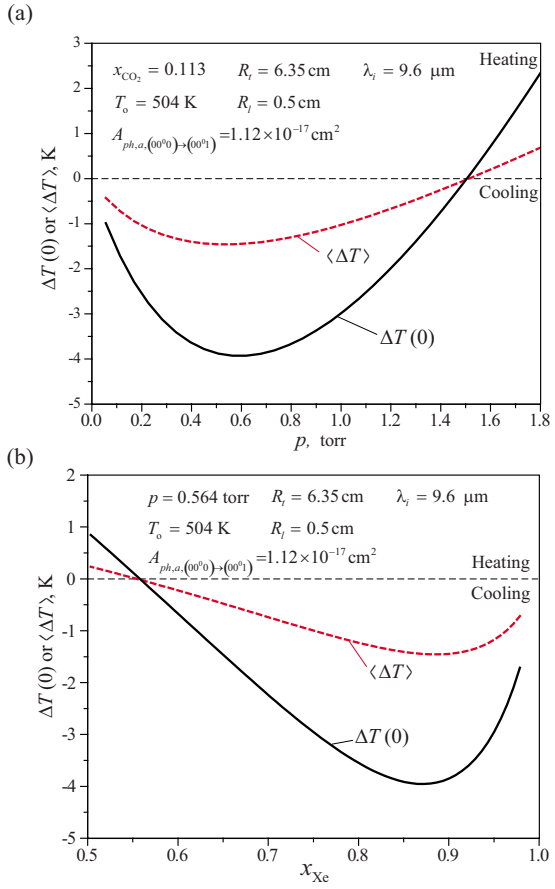

FIG. 3. (Color online) Variations in cooling with respect to (a) total gas pressure p and (b) Xe mole fraction x_{Xe}.

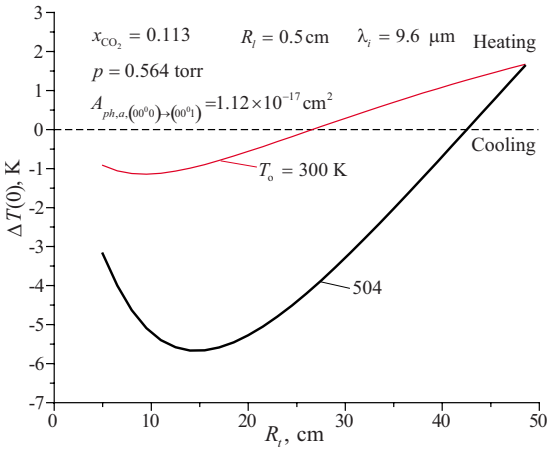

FIG. 4. (Color online) Variations in cooling with respect to cylinder radius R_t at several cylinder temperatures, showing the effect of reabsorption (absorption coefficient and emitted photon path length).

influenced by macroscopic conditions, which in turn influence $\sigma_{\mathrm{ph},a,(00^00)\rightarrow(00^01)}$. Figure 4 shows the variation in cooling with respect to R_t at different cylinder temperatures. Optimal R_t for cooling increases with temperature as reabsorption reduces, as a result of small $\sigma_{\mathrm{ph},a,(00^00)\rightarrow(00^01)}$ at high temperatures.

The large beam radius and larger threshold irradiation required to populate the (00^01) level yield a large laser power. The maximum cooling limit occurs when the (00^01) level is saturated throughout the gas ($R_l=R_t$, i.e., $\beta=1$), so it requires a high laser power. We note that the maximum cooling for $T_o=300$ K ($R_l=R_t=10$ cm, $p=0.67$ torr, and $x_{Xe}=0.89$) is $\Delta T(0)_{max}=8.07$ K (with cooling rate of 317.6 K/s). Also, at the optimal temperature $T_o=504$ K ($R_l=R_t=14$ cm, $p=0.56$ torr, and $x_{Xe}=0.89$), the maximum cooling limit is $\Delta T(0)_{max}=44.9$ K (with cooling rate of 2427 K/s).

IV. CONCLUSION

We analyzed anti-Stokes molecular-gas laser cooling and its enhancement by manipulating population distribution. Deviation of the excited vibrational-level population of CO_2 from the equilibrium population is central in laser cooling enhancement. In this analysis, in order to enhance cooling, we manipulated vibration population distribution by varying incoming photon energies. In particular, irradiation with a 9.6 μm wavelength for resonance with (02^00) improves cooling performance by increasing the population of the (00^01) level. The availability of tunable dye lasers to achieve the desired wavelength makes it possible to target vibrational population inversions for the most effective cooling. With this ability to select the excitation, we have addressed the optimal cooling of CO_2. The desired nonequilibrium population distribution for laser cooling can be achieved by resonance with other energy carriers, such as electrons or phonons. Thus, a possible extension of population manipulation for cooling enhancement is to increase the population of (10^00) by low-energy electron impaction along with 10.6 μm laser irradiation, which would improve cooling through the large population of the (00^01) level.[33,34] Also, the internal vibrational energy of the bounding solid (phonon) can excite the vibrational energy level of gas molecules adsorbed on the solid surface.[35] Therefore finding the relaxation channel of phonons resonating with excited energy levels is another possible extension to improve cooling.

Optimal macroscopic conditions (T, p, and x_{Xe}) allow for large excited-level population through control of species diffusion and kinetics of the excited vibration levels, which improves cooling with hindered energy transport. Inclusion of reabsorption determines the optimal geometry. With (02^00) excitation and selection of gas conditions and geometry, we predict enhanced anti-Stokes cooling of CO_2–Xe gas even at or around room temperature. Then cooling is effective at low pressures, but the cooling rate is fast and it is nonmechanical, with possible applications in space telescope or satellite and where there is a need for fast cooling of not easily accessible regions.

[1] W. Neuhauser, M. Hohenstatt, P. Toschek, and H. Dehmelt, Phys. Rev. Lett. **41**, 233 (1978).
[2] D. Wineland, R. E. Drullinger, and F. L. Walls, Phys. Rev. Lett. **40**, 1639 (1978).
[3] P. S. Julienne and F. H. Mies, J. Opt. Soc. Am. B **6**, 2257 (1989).
[4] W. D. Phillips, Rev. Mod. Phys. **70**, 721 (1998).
[5] J. T. Bahns, W. C. Stwalley, and P. L. Gould, J. Chem. Phys. **104**, 9689 (1996).
[6] S. Banerjee and G. Gangopadhyay, J. Chem. Phys. **123**, 114304 (2005).
[7] M. D. Di Rosa, Eur. Phys. J. D **31**, 395 (2004).
[8] L. D. Carr, D. DeMille, R. V. Krems, and J. Ye, New J. Phys. **11**, 055049 (2009).
[9] D. R. Siebert, F. R. Grabiner, and G. W. Flynn, J. Chem. Phys. **60**, 1564 (1974).
[10] F. G. Gebhardt and D. C. Smith, Appl. Phys. Lett. **20**, 129 (1972).
[11] N. Djeu and W. T. Whitney, Phys. Rev. Lett. **46**, 236 (1981).
[12] J. Kim, A. Kapoor, and M. Kaviany, Phys. Rev. B **77**, 115127 (2008).
[13] G. Herzberg, *Infrared and Raman Spectra of Polyatomic Molecules*, Molecular Spectra and Molecular Structure Vol. II (Van Nostrand, New York, 1945).
[14] W. Duley, *Lasers: Effects and Applications* (Academic, London, 1976).
[15] P. K. Cheo, IEEE J. Quantum Electron. **4**, 587 (1968).
[16] J. C. Stephenson, R. E. Wood, and C. B. Moore, J. Chem. Phys. **54**, 3097 (1971).
[17] N. B. Vargaftik, *Handbook of Thermal Conductivity of Liquids and Gases* (CRC, Boca Raton, FL, 1994).
[18] C. Dang, J. Reid, and B. K. Garside, Appl. Phys. B: Lasers Opt. **27**, 145 (1982).
[19] L. Doyennette, M. Margottin-Maclou, H. Gueguen, A. Carion, and L. Henry, J. Chem. Phys. **60**, 697 (1974).
[20] R. B. Bird, W. E. Stewart, and E. N. Lightfoot, *Transport Phenomena* (Wiley, New York, 1960).
[21] F. I. Irwine, *Handbook of Heat Transfer* (McGraw-Hill, New York, 1998).
[22] M. Kaviany, *Heat Transfer Physics* (Cambridge University Press, New York, 2008).
[23] Z. Liang and H. L. Tsai, J. Mol. Spectrosc. **252**, 108 (2008).
[24] T. D. Kolomiĭtsova, A. V. Lyaptsev, and D. N. Shchepkin, Opt. Spectrosc. **88**, 648 (2000).
[25] R. N. Schwartz, Z. I. Slawsky, and K. F. Herzfeld, J. Chem. Phys. **20**, 1591 (1952).
[26] V. V. Nevdakh, L. N. Orlov, and N. S. Leshenyuk, J. Appl. Spectrosc. **70**, 276 (2003).
[27] L. D. Landau and E. Teller, in *Collected Papers of L. D. Landau*, edited by D. ter Haar (Gordon and Breach, New York/Science, New York/Pergamon, New York, 1965), p. 147; Phys. Z. Sowjetunion **10**, 34 (1936).
[28] C. B. Moore, R. E. Wood, B. L. Hu, and J. T. Yardley, J. Chem. Phys. **46**, 4222 (1967).

[29]J. T. Yardley and C. B. Moore, J. Chem. Phys. **46**, 4491 (1967).
[30]R. C. Hilborn, Am. J. Phys. **50**, 982 (1982).
[31]C. K. N. Patel, Phys. Rev. **136**, A1187 (1964).
[32]X. L. Ruan and M. Kaviany, Phys. Rev. B **73**, 155422 (2006).
[33]B. L. Whitten and N. F. Lane, Phys. Rev. A **26**, 3170 (1982).
[34]K. H. Kochem, W. Sohn, N. Hebel, K. Jung, and H. Ehrhardt, J. Phys. B **18**, 4455 (1985).
[35]V. P. Zhdanov, Theor. Exp. Chem. **16**, 188 (1980).